Journal of Solid State Chemistry 183 (2010) 3017–3022

Contents lists available at ScienceDirect

Journal of Solid State Chemistry

journal homepage: www.elsevier.com/locate/jssc

Solid-state NMR study of geopolymer prepared by sol–gel chemistry

Yi-Ling Tsai [a], John V. Hanna [b], Yuan-Ling Lee [c,*,1], Mark E. Smith [b,*,2], Jerry C.C. Chan [a,*,3]

[a] Department of Chemistry, National Taiwan University, No. 1, Sec. 4, Roosevelt Road, Taipei 10617, Taiwan ROC
[b] Department of Physics, The University of Warwick, Coventry CV4 7AL, United Kingdom
[c] Graduate Institute of Clinical Dentistry, National Taiwan University and Hospital, No. 1, Changde Street, Taipei 10048, Taiwan ROC

ARTICLE INFO

Article history:
Received 21 May 2010
Received in revised form
27 September 2010
Accepted 4 October 2010
Available online 13 October 2010

Keywords:
Geopolymer
Kaolinite
Sol–gel method
Aluminosilicates

ABSTRACT

Geopolymers are a new class of materials formed by the condensation of aluminosilicates and silicates obtained from natural minerals or industrial wastes. In this work, the sol–gel method is used to synthesize precursor materials for the preparation of geopolymers. The geopolymer samples prepared by our synthetic route have been characterized by a series of physical techniques, including Fourier-transform infrared, X-ray diffraction, and multinuclear solid-state NMR. The results are very similar to those obtained for the geopolymers prepared from natural kaolinite. We believe that our synthetic approach can offer a good opportunity for the medical applications of geopolymer.

1. Introduction

Geopolymers are a new class of network materials with amorphous to semi-crystalline nature [1], which can be formed by the condensation of aluminosilicates and silicates under alkaline conditions. Geopolymers possess excellent mechanical properties, fire resistance and chemical durability. Furthermore, it has also been reported that geopolymers can be used for permanent encapsulation of toxic metals [2,3]. As potentially revolutionary materials for a number of applications, geopolymers have been under an active investigation in recent years [4,5].

The key processes involved in the synthesis of geopolymers include [6–8]: (i) the calcination of kaolinite to form the metakaolinite; (ii) the dissolution and hydrolysis of metakaolinite or similar aluminosilicate precursors to generate the species of $Al(OH)_4^-$ and $Si(O_n(OH)_{4-n})$; (iii) the condensation of these species to build up the geopolymeric network. Since the pioneering work of Davidovits [9], considerable research effort has been and continues to be directed to this area, due to the wide range of potential applications of geopolymers. The mechanistic aspect of the formation process of geopolymer is also an interesting issue. The reactions between metakaolinite and alkaline silicate solutions have been studied by a number of techniques, including thermal analysis [10,11], Fourier-transform infrared (FT-IR), and solid-state nuclear magnetic resonance (NMR) [12–14]. However, the mechanisms involved in the processes of dissolution, hydrolysis and condensation remain poorly understood.

The potential applications of geopolymers are not limited to being used as construction materials. Composite materials formed of geopolymer and calcium phosphate have been suggested as a biocompatible synthetic bone replacement material [15–17]. Encouragingly, Oudadesse et al. have shown that there are no aluminum ions released from their geopolymer samples after soaking in simulated body fluid (SBF) or *in vivo* implantation in rabbit thighbone [18]. However, typical starting materials for the melt-quench preparation of geopolymers include industrial wastes [3,14,19], calcined clays [10,20], melt–quenched aluminosilicates [21], natural materials [22], or mixtures of these materials [23]. Therefore, it is very difficult to employ the conventional approach to prepare geopolymers which can meet the stringent requirements for medical applications. It is of great interest to develop a synthetic protocol to prepare geopolymers with well defined chemical composition. In this work, we have adopted the sol–gel method for the preparation of geopolymers. The geopolymer samples prepared from our sol–gel route have been characterized by the X-ray diffraction technique (XRD), FT-IR, and multinuclear (^{23}Na, ^{27}Al, and ^{29}Si) solid-state NMR spectroscopy. The results show that the geopolymers prepared by our synthetic approach have rather similar mechanical and spectroscopic properties to those prepared conventionally from natural kaolinite.

* Corresponding authors.
E-mail addresses: yuanlinglee@ntu.edu.tw (Y.-L. Lee), M.E.Smith.1@warwick.ac.uk (M.E. Smith), chanjcc@ntu.edu.tw (J.C.C. Chan).
[1] Tel.: +886 2 23123456x67400.
[2] Tel.: +44 24 76522380/523965.
[3] Tel.: +886 2 33663895.

0022-4596/$ - see front matter © 2010 Elsevier Inc. All rights reserved.
doi:10.1016/j.jssc.2010.10.008

2. Experimental

2.1. Sample preparation

Crystalline natural kaolinite was obtained from Fluka. All other precursors were obtained from Sigma-Aldrich Organics and used as received without any purification.

Synthetic kaolinites: synthetic kaolinite (SK) was prepared following the procedure reported earlier [24]. To prepare the precursor for SK, 6 g of aluminum *iso*-propoxide ($Al(^iPO)_3$) and 16.35 mL of tetraethyl orthosilicate (TEOS) were added into 800 mL of deionized (DI) water at regular time intervals. The solution was further agitated for 24 h to complete the precipitation process. The mixture was dried at 60 °C for 36 h and ground. Three samples prepared with different time intervals for the reagent addition (see Table 1) were used as precursor for an SK preparation, and they are henceforth referred to as SKP-A, SKP-B, and SKP-C. For the sample of SKP-D, the amount of $Al(^iPO)_3$ and TEOS was increased to 7.2 g and 19.62 mL, respectively. To prepare the SK samples, each batch of the SKP sample (2.5 g) was then mixed with 10 mL of 0.1 M KOH solution. The mixture was hydrothermally treated at 240 °C in an autoclave with a duration varying from 48 h to one week. The SK samples obtained were labeled on the basis of their heat treatment duration. That is, the SK sample after hydrothermal treatment for 2 days is referred to as SK-2d. After the heat treatment, the product was collected by suction filtration and dried at 60 °C for 24 h.

Activator solutions: the activator solution to be used for the synthesis of the geopolymer was prepared by adding 10.96 g of NaOH pellets into 100 g of pre-cooled sodium silicate solution, resulting in an Na_2O/SiO_2 molar ratio of 0.7. The activator solutions were well mixed for at least 24 h before use.

Geopolymer: each batch of the SK sample (2 g) was placed in an alumina crucible and calcined at 700 °C for 10 h to form the so-called meta-SK (MSK) compound. The sample was then cooled down to room temperature at 1 °C/min. The target geopolymer was prepared by blending 100 mg of MSK sample with the activator solution on a Teflon plate to obtain the paste with the molar ratio of Si:Al=2.5:1. The mixture was then sealed and aged at 60 °C for 22 h, followed by air drying for another 24 h. The same procedure was carried out for the preparation of other geopolymers from different Si–Al sources.

2.2. Sample characterization

XRD analysis was performed on a PANalytical X'Pert Pro diffractometer, using Cu-$K\alpha$ radiation (λ=1.540598 Å). The FT-IR spectra were measured on Nicolet Magna-IR 760 Fourier-transform spectrometer.

Solid-state NMR: all the ^{23}Na and ^{27}Al NMR experiments were measured on a Bruker Avance 400 NMR spectrometer equipped with a commercial 4-mm probe, whereas ^{29}Si NMR experiments were carried out on Varian 300 Infinity Plus spectrometer, using a 7.5 mm probe. The ^{23}Na, ^{27}Al, and ^{29}Si magic-angle spinning (MAS) measurements were carried out at frequencies of 105.5, 104.1, and 59.5 MHz, respectively. All spectra were measured at room temperature. The sample was confined to the middle one-third of the rotor volume, using Teflon spacers. The spinning frequency variation was limited to $\pm$3 Hz using a commercial pneumatic control unit. Chemical shifts were externally referenced to 1.0 M of $Al(NO_3)_3$ aqueous solution and tetramethylsilane (TMS) for ^{27}Al and ^{29}Si, respectively. For the measurements of the ^{27}Al (I=5/2) spectra, nonselective π pulses of 12 μs were calibrated on the solution standard, from which the flip angle of the excitation pulse was set to fulfill the condition of $(I+1/2)\omega_{rf}t_p \leq \pi/6$. The recycle delays were set to 3 s. The spinning frequency was set to 12 kHz. For the ^{29}Si MAS experiments, all the Bloch-decay spectra were measured at a spin rate of 4 kHz without proton decoupling. The flip angle was set to $\pi/4$ (2.5 μs) and the recycle delay was set to 30 s.

Table 1
Preparation conditions of SKP samples.

	Addition time interval (min)	Total amount of reactants
SKP-A	10	[1.2 g of $Al(^iPO)_3$+3.27 ml TEOS] × 5 times
SKP-B	30	[1.2 g of $Al(^iPO)_3$+3.27 ml TEOS] × 5 times
SKP-C	60	[1.2 g of $Al(^iPO)_3$+3.27 ml TEOS] × 5 times
SKP-D	10	[1.2 g of $Al(^iPO)_3$+3.27 ml TEOS] × 6 times

3. Results and discussion

3.1. Preparation of synthetic kaolinite

Table 1 summarizes the preparation conditions of four SKPs to optimize the time interval for the addition of $Al(^iPO)_3$ and TEOS. The ^{29}Si MAS NMR spectra of the four SKP samples are very similar and each spectrum has a single featureless signal with a linewidth of 1500 Hz and the chemical shift is about −100 ppm. The corresponding ^{27}Al MAS NMR spectra have two major resonances, which could be assigned to Al^{IV} and Al^{VI} (see Supporting Information). The relative ratios of the signal integrals of Al^{VI} and Al^{IV} are 1.92, 1.60, 1.78, and 1.38 for SKP-A, SKP-B, SKP-C, and SKP-D, respectively.

Fig. 1 shows the ^{27}Al and ^{29}Si MAS NMR spectra of the SK-2d samples. The ^{27}Al and ^{29}Si MAS NMR spectra of natural kaolinite were also measured for comparison, from which the ^{27}Al and ^{29}Si NMR signals at 0 and −92 ppm, respectively, could be taken as the spectral markers of kaolinite (Fig. 1a). Interestingly, the ^{29}Si spectra of the SK-2d samples have rather distinctive features. From the ^{29}Si spectra, all the SK-2d samples contain a resonance at −92 ppm, which provides an evidence for the formation of kaolinite. The line shapes of the spectra of SK-B-2d and SK-C-2d are similar to each other. According to the peak intensity at −92 ppm, we conclude that the SK-D-2d sample has the lowest content of kaolinite. The minor component at ca. −98 ppm is assigned to Q^4(1Al), whereas the very broad peak at −108 ppm is assigned to Q^4(0Al) [25,26]. On the other hand, the SK-2d samples show two resonances at 0 and 50 ppm in the ^{27}Al MAS NMR spectra, which is similar to what have been observed for the SKP samples. Nonetheless, the ratio of Al^{VI}/Al^{IV} increased substantially after hydrothermal treatment, which gives strong support to the scenario that the structural transformation of an SKP (amorphous) produces kaolinite. In addition, there are two minor peaks in the AlO_4 region of the ^{27}Al spectrum, which is quite similar to what have been reported for pyrophyllite [27,28]. Accordingly, the peaks at 65 and 51 ppm are assigned to the Q^3(3Si) and Q^4(4Si) units, respectively [25]. The more de-shielded peak, in particular, is assigned to the hydroxylated aluminum tetrahedral layers [26]. The FT-IR spectra of the SK-2d samples are shown in Fig. 2, together with that measured for natural kaolinite. The spectrum of kaolinite has two hydroxyl absorption bands at 3619 and 3694 cm^{-1}, as well as a characteristic band at 913 cm^{-1} due to the Al–OH vibration. Using these spectral markers, it can be inferred that all the SK samples contain kaolinite. Because the OH^- bands are more resolved in the samples SK-2d-A and SK-2d-D, apparently, the crystallinity of these two samples are somewhat better.

Selected samples of SK-2d, SK-4d, and SK-7d were characterized by XRD measurements (data not shown). The results indicate that sample crystallinity is the best for the SK-7d samples. The characteristic diffraction peaks of natural kaolinite are located at around

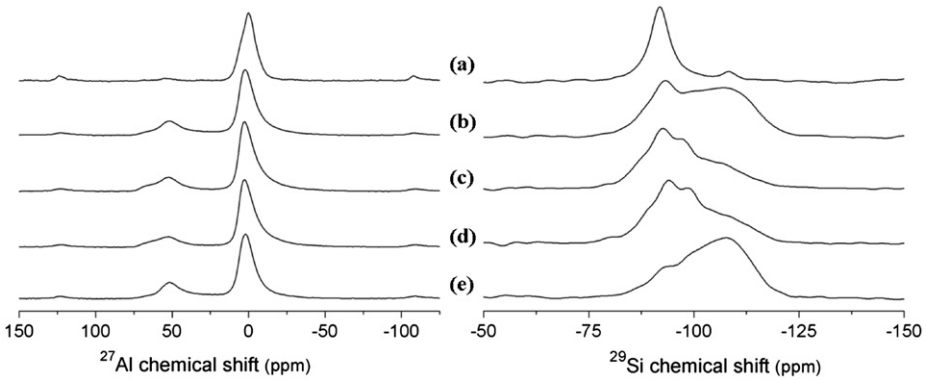

Fig. 1. ^{27}Al (left column) and ^{29}Si (right column) MAS spectra of (a) natural kaolinite, (b) SK-A-2d, (c) SK-B-2d, (d) SK-C-2d, and (e) SK-D-2d.

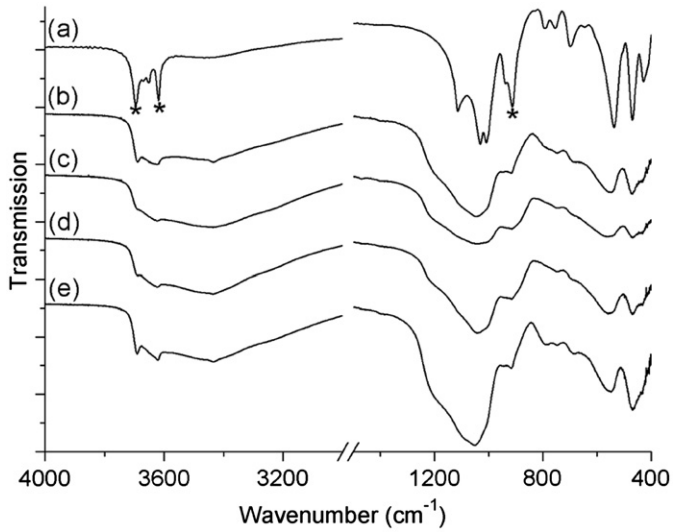

Fig. 2. FT-IR spectra of (a) natural kaolinite, (b) SK-A-2d, (c) SK-B-2d, (d) SK-C-2d, and (e) SK-D-2d. The asterisks indicate the characteristic absorption of kaolinite, viz. OH vibration bands at 3700 and 3620 cm^{-1}, and the Al–OH absorption band at 920 cm^{-1}.

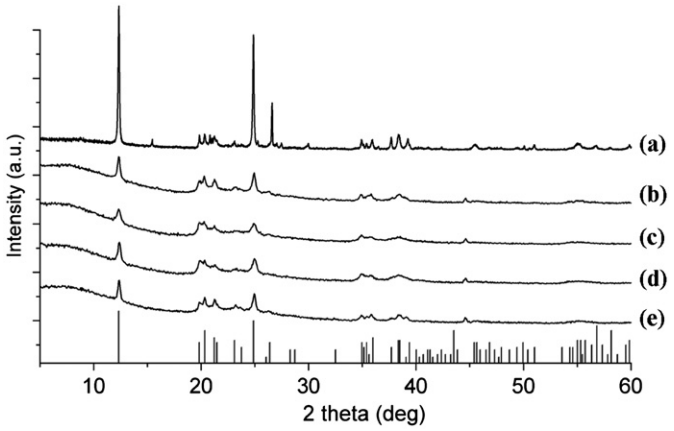

Fig. 3. XRD patterns of (a) natural kaolinite (b) SK-A-7d, (c) SK-B-7d, (d) SK-C-7d, and (e) SK-D-7d. The calculated pattern for kaolinite (JCPDS 140164) is shown in the bottom.

13° and 25° (2θ), which correspond to the (0 0 1) and (0 0 2) planes, respectively. These two peaks have been assigned to the layer structure of kaolinite [29–32]. Fig. 3 shows the XRD patterns of the SK-7d samples. Our SK-7d samples show a similar pattern to the natural kaolinite, but with weaker intensities. From the linewidths of the diffraction peaks, we conclude that the crystallinity of the samples of SK-A-7d and SK-D-7d is slightly better than that of SK-B-7d and SK-C-7d. This observation is consistent with the FT-IR data. In summary, the time interval for the addition of the starting materials (Table 1) has a great influence to the speciation of the product and the sample SK-A has the best sample quality according to the NMR, FT-IR, and XRD data. As a result, we will focus on the SK-A sample in the subsequent discussion.

Fig. 4 shows the ^{27}Al and ^{29}Si MAS NMR spectra of the SK-A-2d to SK-A-7d samples. The longer the heat treatment period, the more the spectral features of the SK-A sample resemble those of the natural kaolinite. Furthermore, the ratio of the Al^{VI}/Al^{IV} species increases with the hydrothermal time. The relative amount of four- and six-coordinated aluminum species extracted from the ^{27}Al MAS NMR spectra are plotted in Fig. 5. It is clearly shown that the increase in the Al^{VI} intensity mirrors the decrease in Al^{IV}. Therefore, we conclude that an appreciable amount of Al^{IV} had been converted to Al^{VI} during the hydrothermal treatment. ^{29}Si chemical shifts are very sensitive to the change in the coordination of the silicon atom. Usually, the Q^0 species, which denote silicate ions with no bridging oxygen atoms, have typical ^{29}Si chemical shifts of about −65 ppm. For each of the additional bridging oxygen, a shift of about 10 ppm to the shielded region occurs [33]. That is, the ^{29}Si chemical shift of the fully polymerized silicon species (Q^4) is about −110 ppm. In addition, the substitution by an Al of each of the four silicons surrounding the central Si would result in a shift towards the deshielding region. In other words, the ^{29}Si chemical shift of $Q^4(n\mathrm{Al})$ will increase as the number n increases from 0 to 4. The ^{29}Si MAS NMR spectra of our SK-A samples were deconvoluted. Fig. 6a shows the experimental and the deconvoluted ^{29}Si MAS spectra of SK-A-7d, in which the line shape could be simulated, using two Gaussian peaks. The chemical shifts of the two major components are found to be −92 and −107 ppm, which can be assigned to $Q^4(2\mathrm{Al})$ and $Q^4(0\mathrm{Al})$, respectively [26]. Fig. 6b plots the relative signal integrals of the two components against the hydrothermal period. As the period increases, the signal integral of the peak component at −92 ppm increases at the expense of that at −107 ppm. In comparison with the ^{29}Si MAS NMR spectrum of an SKP-A (see Fig. 4), we suggest that during the hydrothermal treatment, the kaolinite framework, i.e. $Q^4(2\mathrm{Al})$–AlO_6 species, is formed via the substitution of an Si by an Al in two steps.

Step 1: $2Q^4(1\mathrm{Al}) \rightarrow Q^4(2\mathrm{Al}) + Q^4(0\mathrm{Al})$.
Step 2: $Q^4(0\mathrm{Al}) + 2Al^{IV} \rightarrow Q^4(2\mathrm{Al})$.

The first step accounts for the spectral difference between the SKP-A and SK-A-2d samples, whereas the second step could

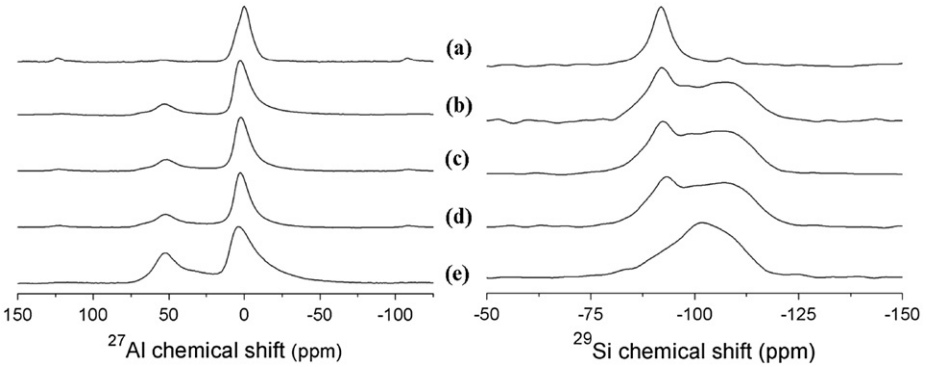

Fig. 4. ^{27}Al (left column) and ^{29}Si (right column) MAS spectra of the (a) natural kaolinite, (b) SK-A-7d, (c) SK-A-4d, (d) SK-A-2d, and (e) SKP-A.

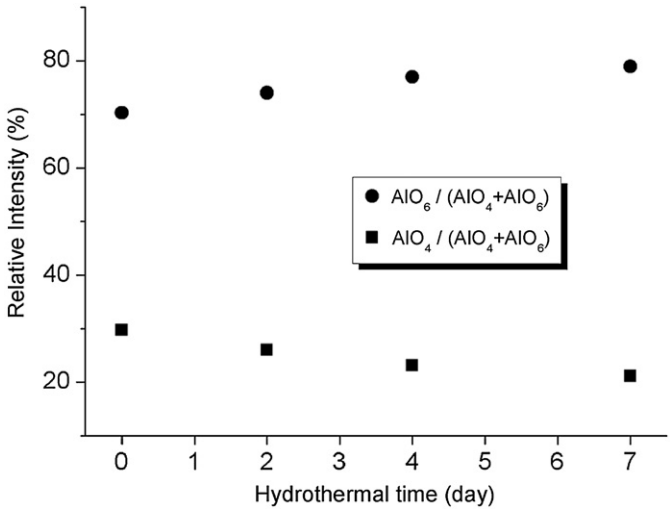

Fig. 5. Relative amount of AlO_4 and AlO_6 obtained from the deconvolution of the ^{27}Al NMR spectra of the SK-A samples. Minor effects due to the difference in quadrupolar interaction are ignored.

rationalize the minor spectral change, when the hydrothermal treatment increases from 2 to 7 days (see Fig. 6b).

3.2. Preparation of geopolymer

3.2.1. Calcination of synthetic kaolinite

To prepare geopolymer, the SK samples must first be calcined at 700 °C for 10 h. The obtained MSK samples were characterized by FT-IR, XRD, and NMR. After calcination, sample dehydration is evident by the disappearance of the OH^- stretching peaks at 3700 and 920 cm^{-1} (see Supporting Information, S-2). The XRD measurements show that the metakaolinite sample, which was obtained by calcinations of the natural kaolinite at 700 °C for 10 h, contains some residual crystalline phase. Similar results were observed for the MSK-A-7d sample (see Supporting Information). On the basis of the features observed in the ^{27}Al MAS NMR spectrum (Fig. 7), we find that the metakaolinite sample contains four-, five-, and six-coordinated aluminum species. In comparison, the AlO_6 species is somewhat overrepresented in our MSK-A samples. On the other hand, the ^{29}Si MAS NMR spectrum of metakaolinite exhibits a major resonance at −102 ppm and another minor resonance at −108 ppm, which can be assigned to a layer structure of Q^3 and the residual quartz, respectively [26]. The line shapes of the spectra of the MSK-A series have considerable dependence on the hydrothermal time. As shown in Fig. 7, the ^{29}Si MAS NMR spectra of MSK-A-4d and -7d can be simulated by two Gaussian peaks, which are located at −102 and −109 ppm, whereas the ^{29}Si spectrum of an MSK-A-2d has three different components at −92, −98, and −106 ppm. Overall, the spectral features of the MSK-A-7d and metakaolinite are very similar.

3.2.2. Synthesis and characterization of geopolymer

The geopolymer sample was prepared by mixing the MSK-A samples with the activator solution. The mixture was then set at 60 °C for 22 h. As discussed above, the three MSK-A samples are structurally different. Interestingly, the spectral properties of the ^{27}Al and ^{29}Si NMR spectra of the resulting geopolymers prepared from the metakaolinite and MSK-A are almost the same. Furthermore, the microhardness was found to be approximately the same for all the geopolymer samples (data not shown). Referring to Fig. 8, the ^{27}Al MAS NMR spectrum has a single resonance at around 57 ppm, which is readily assigned to tetrahedral aluminum species. This result is in line with the expectation that most of the five- and six-coordinated aluminum species of the MSK-A samples will condense to form the three-dimensional geopolymer network, which mainly comprises four-coordinate aluminum species. For the ^{29}Si MAS NMR spectra, the major resonance of the geopolymer is located at −94 ppm, which can be assigned to Q^4(1Al) and/or Q^4(2Al) species [26]. Recently, Lacaillerie and co-workers have reported a systematic study on the geopolymer samples prepared from pure kaolinite and from kaolin containing other minerals [26]. It has been concluded that kaolin containing as much as 30% of secondary minerals, such as an illite can still be used to prepare geopolymer. In another study of geopolymer prepared by the sol–gel method (Si/Al ratio close to 1), the starting materials were dried and calcined without any hydrothermal treatment [32]. Together with our results, we believe that geopolymer can be formed from different sources of aluminosilicate with a large variety of chemical composition. Additional works are required to identify the key steps in the preparation of geopolymer.

4. Conclusion

We have successfully developed a preparation protocol for geopolymer. In our approach, the sol–gel method is used to prepare the precursor material for the subsequent geopolymer preparation. Although our synthetic kaolinite has somewhat different spectroscopic properties from the natural kaolinite, the geopolymer prepared from both sources exhibit similar spectroscopic properties. Compared with the traditional approach that employed natural kaolinite as the starting material, our synthetic approach can prepare geopolymer with more diversified chemical composition. We believe that our synthetic approach can offer a good opportunity for the medical applications of geopolymer.

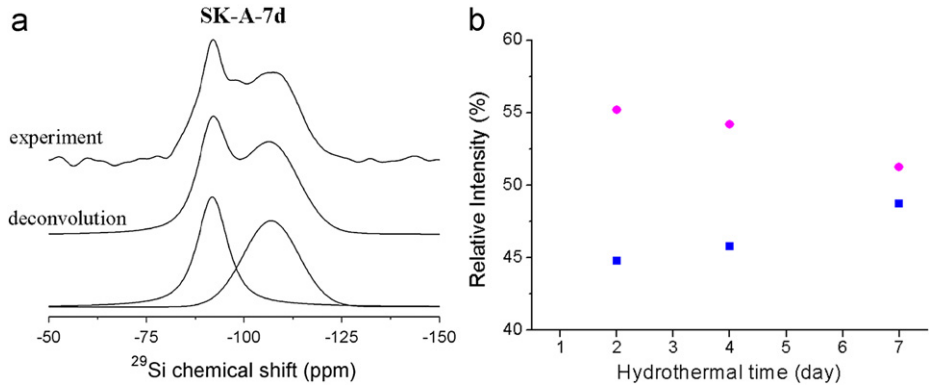

Fig. 6. (a) Experimental and deconvolution ^{29}Si spectra of an SK-A-7d. (b) Relative intensity of the signals at −92 ppm (■) and −106.9 ppm (●) obtained for the SK-A-2d to SK-A-7d samples.

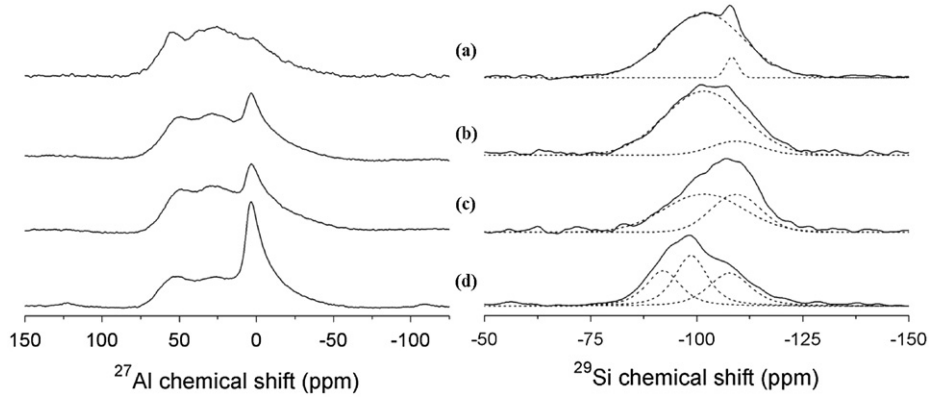

Fig. 7. ^{27}Al and ^{29}Si MAS spectra of (a) metakaolinite, (b) MSK-A-7d, (c) MSK-A-4d, and (d) MSK-A-2d.

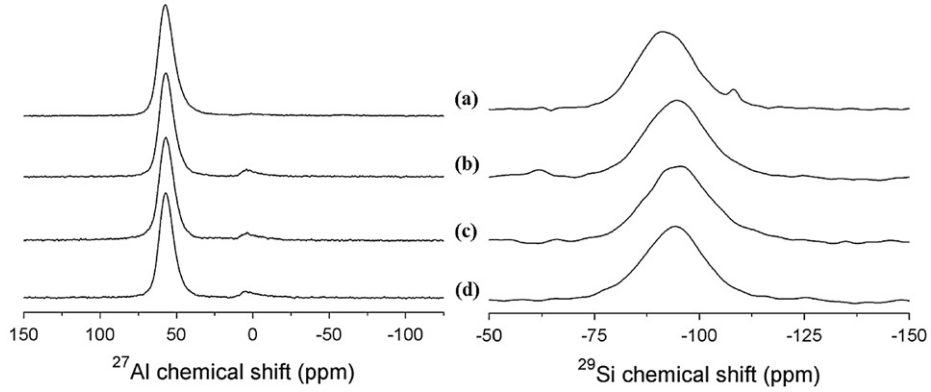

Fig. 8. ^{27}Al and ^{29}Si MAS spectra of the geopolymer samples prepared from (a) metakaolinite, (b) MSK-A-7d, (c) MSK-A-4d, and (d) MSK-A-2d.

Acknowledgments

This work was supported by grants from the National Science Council and the Ministry of Education. The visit of YLT to the University of Warwick was made possible by the Graduate Students Study Abroad program of National Science Council. The NMR infrastructure at Warwick is funded through a variety of sources, including EPSRC, the HEFCE, and the University of Warwick as well as through the Science City Advanced Materials project supported by Advantage West Midlands (AWM) and part funded by the European Regional Development Fund (ERDF). MES and JVH are grateful to all their sponsors.

Appendix A. Supporting information

Supplementary data associated with this article can be found in the online version at doi:10.1016/j.jssc.2010.10.008.

References

[1] J. Davidovits, Therm. Anal. 37 (1991) 1633–1656.
[2] J.G.S. van Jaarsveld, J.S.J. van Deventer, L. Lorenzen, Miner. Eng. 10 (1997) 659–669.
[3] J.G.S. van Jaarsveld, J.S.J. van Deventer, A. Schwartzman, Miner. Eng. 12 (1999) 75–91.

[4] T.W. Cheng, J.P. Chiu, Miner. Eng. 16 (2003) 205–210.
[5] Y.S. Zhang, W. Sun, Q.L. Chen, L. Chen, J. Hazardous Mater. 143 (2007) 206–213.
[6] L. Weng, K. Sagoe-Crentsil, J. Mater. Sci. 42 (2007) 2997–3006.
[7] K. Sagoe-Crenstil, L. Weng, J. Mater. Sci. 42 (2007) 3007–3014.
[8] Y.J. Zhang, Y.L. Zhao, H.H. Li, D.L. Xu, J. Mater. Sci. 43 (2008) 7141–7147.
[9] J. Davidovits, J. Therm. Anal. 35 (1989) 429–441.
[10] H. Rahier, B. van Mele, M. Biesemans, J. Wastiels, X. Wu, J. Mater. Sci. 31 (1996) 71–79.
[11] H. Rahier, W. Simons, B. VanMele, M. Biesemans, J. Mater. Sci. 32 (1997) 2237–2247.
[12] A. Palomo, M.T. Blanco-Varela, M.L. Granizo, F. Puertas, T. Vazquez, M.W. Grutzeck, Cem. Concr. Res. 29 (1999) 997–1004.
[13] V.F.F. Barbosa, K.J.D. MacKenzie, C. Thaumaturgo, Int. J. Inorg. Mater. 2 (2000) 309–317.
[14] M.R. Rowles, J.V. Hanna, K.J. Pike, M.E. Smith, B.H. O'Connor, Appl. Magn. Reson. 32 (2007) 663–689.
[15] A.C. Derrien, H. Oudadesse, J.C. Sangleboeuf, P. Briard, A. Lucas-Girot, J. Therm. Anal. Calorimetry 75 (2004) 937–946.
[16] H. Oudadesse, A.C. Derrien, M. Lefloch, J. Therm. Anal. Calorimetry 82 (2005) 323–329.
[17] H. Oudadesse, A.C. Derrien, M. Mami, S. Martin, G. Cathelineau, L. Yahia, Biomed. Mater. 2 (2007) S59–S64.
[18] H. Oudadesse, A.C. Derrien, M. Lefloch, J. Davidovits, J. Mater. Sci. 42 (2007) 3092–3098.
[19] A. Palomo, M.W. Grutzeck, M.T. Blanco, Cem. Concr. Res. 29 (1999) 1323–1329.
[20] A. Palomo, F.P. Glasser, Br. Ceram. Trans. J. 91 (1992) 107–112.
[21] J.P. Hos, P.G. McCormick, L.T. Byrne, J. Mater. Sci. 37 (2002) 2311–2316.
[22] H. Xu, J.S.J. van Deventer, Int. J. Miner. Process. 59 (2000) 247–266.
[23] H. Xu, J.S.J. van Deventer, G.C. Lukey, Ind. Eng. Chem. Res. 40 (2001) 3749–3756.
[24] C.R. De Kimpe, H. Kodama, R. Rivard, Clays Clay Miner. 29 (1981) 446–450.
[25] T. Takahashi, T. Ohkubo, K. Suzuki, Y. Ikeda, Microporous Mesoporous Mater. 106 (2007) 284–297.
[26] F. Zibouch, H. Kerdjoudj, J.-B. d.E. d. Lacaillerie, H.V. Damme, Appl. Clay Sci. 43 (2009) 453–458.
[27] R.L. Frost, P.F. Barron, J. Phys. Chem. 88 (1984) 6206–6209.
[28] S.K. Lee, J.F. Stebbins, C.A. Weiss, R.J. Kirkpatrick, Chem. Mater. 15 (2003) 2605–2613.
[29] G.W. Brindley, K. Robinson, Nature 156 (1945) 661–662.
[30] R.F. Giese, Rev. Mineral. Geochem. 19 (1988) 29–66.
[31] D.R. Collins, C.R.A. Catlow, Acta Crystallogr. Sect. B: Struct. Sci. 47 (1991) 678–682.
[32] X.-M. Cui, L.-P. Liu, G.-J. Zheng, R.-P. Wang, J.-P. Lu, J. Non-Cryst. Solids 356 (2010) 72–76.
[33] K.J.D. MacKenzie, M.E. Smith, in: Multinuclear Solid-State NMR of Inorganic Materials, PERGAMON, 2002.